Vol 17 No 2, February 2008
1674-1056/2008/17(02)/0655-07

Chinese Physics B

© 2008 Chin. Phys. Soc.
and IOP Publishing Ltd

Ab initio study of oxygen-vacancy $LaAlO_3(001)$ surface*

Tang Jin-Long(唐金龙), Zhu Jun(朱 俊)†, Qin Wen-Feng(秦文峰),
Xiong Jie(熊 杰), and Li Yan-Rong(李言荣)

State Key Laboratory of Electronic Thin Films and Integrated Devices, University of Electronic Science and Technology of China, Chengdu 610054, China

(Received 8 March 2007; revised manuscript received 4 September 2007)

Density functional theory is used to investigate the surface structures and the energies of two possible terminated $LaAlO_3$ (001) surfaces with oxygen vacancies, i.e. LaO- and AlO_2-terminated surfaces. The large displacements of ions, deviated from their crystalline sites, can lead to the formation of the surface rumpling. From thermodynamics analysis, the AlO_2-terminated surface with oxygen-vacancies is less stable than the LaO-terminated one. Some states in the gap lie under the Fermi level by about –1eV in the LaO-terminated surface with oxygen vacancies. For the AlO_2-terminated oxygen-vacancy surface, some O 2p states move into the mid-gap region and become partially unoccupied. The two types of termination surfaces exhibit conduction related to oxygen vacancies. Our results can contribute to the application of LAO films to high dielectric constant materials.

Keywords: oxygen vacancy, surface conduction, density functional calculation
PACC: 6170P, 7320A, 7115M

1. Introduction

One of the key challenges to semiconductor technology in the coming years will be the replacement of SiO_2 as a gate dielectric in microelectronic devices. Because of increasing scaling down of device dimensions, conventional gate oxides will finally reach a critical thickness under which they lose their insulating properties due to tunnelling currents. The replacement of SiO_2 by oxides with a dielectric constant κ higher than that of SiO_2 can increase the capacitance of the gate stack by using a gate oxide with a greater physical thickness. Lanthanum aluminate ($LaAlO_3$) has recently gained more attention in this context,[1] and it has been really used in devices. $LaAlO_3$ has won the position of candidate gate oxide entirely on its own unique features, such as the measured average dielectric constant as high as about 25 at room temperature,[2] lattice mismatch to Si(001) substrates less than 1%, a gap of around 5.6eV[1], excellent thermal stability at about 2100°C[3] and good value of the interface band offset to Si, and possibility of interfacial-oxide-free growth on Si.[4]

$LaAlO_3$ films are usually fabricated in high vacuum by using different techniques, such as pulsed laser deposition (PLD)[5] and laser molecular beam epitaxy (LMBE),[6] to eliminate possible interface layer which is harmful to MOSFET devices. However, it can result in oxygen vacancy in $LaAlO_3$ films. The high-κ oxides are late to be adopted in CMOS partly because of their high defect concentrations, particularly oxygen vacancies (V_O). This deficiency results in charge trapping, transient threshold voltage shifting, and semiconductor carrier mobility degrading due to remote Coulombic scattering. Therefore, it is necessary to have a good prediction of V_O defect properties. Recently, Xiong *et al*[7] have studied the defects in the bulk of $LaAlO_3$, such as the oxygen vacancy and oxygen interstitial. Pentcheva and Pickett[8] have investigated the oxygen vacancies in the multilayer of LAO/STO. Asthagiri and Sholl[9] have examined the Pt thin films on $LaAlO_3(100)$ surface by using the density functional theory (DFT), and Knizhnik *et al*[10] have investigated the interface of $Si/LaAlO_3$. However, few studies have focused on the defects of $LaAlO_3$ surfaces, such as oxygen vacancies.

The DFT is a powerful calculation tool, which has been successfully used in many fields.[11–17] In

*Project supported by the National Science Fund for distinguished Young Scholars of China (Grant No 50425207).
†Corresponding author. E-mail: junzhu@uestc.edu.cn

the present study, the DFT is used to investigate the atomic and electronic structures of $LaAlO_3(001)$ surfaces with oxygen vacancies. The atomic relaxation and the electron distribution in two termination surfaces of (001) $LaAlO_3$ with oxygen vacancies in the ground state are both studied. The remainder of the present study is arranged as follows. The model of surface structure and the computational details are described in Section 2. Section 3 demonstrates the results of the atomic and electronic structures. Further comparative study is also made in Section 3. The conclusion drawn from the present study is given in Section 4.

2. Model and computational details

We have carried out the self-consistent calculation of total energy within the framework of density functional theory[18,19] by using the Vanderbilt ultrasoft-pseudopotential scheme.[20] The pseudopotentials include La $5s^2$ $5p^6$ $5d^1$ $6s^2$, Al $3s^2$ $3p^1$ and O $2s^2$ $2p^4$ as valence electrons. The electron wavefunctions are expanded in a plane-wave basis set including a plane wave up to a cutoff energy of 450eV. The cutoff energy is sufficient to obtain well-converged results of these materials. The conjugate-gradient-based approach is used to minimize the sum of eigenvalues. The exchange and the correlation effects are treated by using the local density approximation exchange function LDA-CA-PZ, which is based on the Ceperley and Alder (1980)[21] data as parameterized by Perdew and Zunger (1981).[22] The positions of the ions are determined by minimizing the atomic forces using the Broyden–Fletcher–Goldfarb–Shanno (BFGS) scheme.[23] We use the CASTEP (Cambridge Sequential Total Energy Package) computer code to perform the first-principles DFT calculations.[24]

In the present study, the calculations are performed under a periodic slab geometry. For the type I (LaO terminated) surface, the slab contains five LaO layers and four AlO_2 layers. Similarly, the type II (AlO_2 terminated) slab contains five AlO_2 layers and four LaO layers. In both cases, the slabs are thus four lattices thick, and the vacuum region is ten Angstroms thick. The z-axis is taken to be orthogonal to the surface, and the mirror symmetry with respect to the central layer is imposed in all cases. These slabs are finite in the z-direction but periodic in the x- and y-directions. We remove the oxygen atoms from the surface layer to model the defect surfaces as shown in Fig.1 from the top view of the slabs.

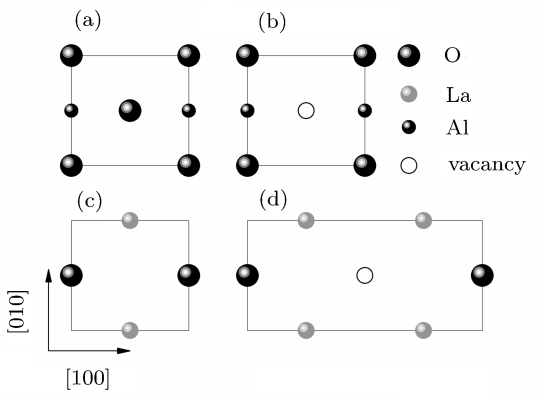


Fig.1. The configuration of two possible terminations (LaO-terminated type I and AlO_2-terminated type II) for the $LaAlO_3(001)$ surfaces from top view: (a) 1×1 cell for perfect surfaces with AlO_2-termination, (b) 1×1 cell for oxygen-vacancy surfaces with AlO-termination, (c) 1×1 cell for perfect surfaces with LaO-termination, (d) 2×1 cell for oxygen-vacancy surfaces with LaO-termination.

The reciprocal space integration is performed by sampling the Brillouin zone[25] of the unit cell with (7,7,1) Pack-Monkhorst net, which can provide the balanced summation in direct and reciprocal spaces.[26] To test the convergence with respect to k point sampling, we have also repeated the calculation for (6,6,1) and (8,8,1) meshes. It is found that the difference in surface energy among the calculations is less than 2%. This k-point set has produced the results within a very reasonable accuracy. The bulk $LaAlO_3$ has a rhombohedral perovskite structure at room temperature, and undergoes a transformation to a simple cubic structure at 710–770K.[27] Since the rhombohedral and the simple cubic phases have very similar structures, the cubic structure is used to study the electrical properties of bulk $LaAlO_3$ and its surface. Besides, current techniques of ferroelectric film growth are workable at a temperature of 700 K, which can further justify our choice of cubic phase. The structure is set up by using our theoretical lattice constant of 0.3754nm obtained by geometric optimization under the condition depicted above, which is close to the parameter obtained from the relation between total energy and volume. The theoretical lattice constant is underestimated by about 1% of the measurement reported (a set of lattice parameter $a = b = c$=0.3788nm, α=β=γ=90.066°),[28] showing that the LDA method usually underestimates

the lattice constants. The error in calculation can be accepted.

3. Results and discussion

3.1. Surface relaxation

The equilibrium positions of atoms are evaluated by the BFGS method through calculating the Hellman–Feynman forces. The final force on each atom is less than 0.01eV/nm. We start from the ideal structure and then relax the atomic positions in the slabs which are measured with respect to the corresponding undistorted bulk $LaAlO_3$, with the full set of symmetries preserved. The pseudopotential representation is in reciprocal space. The relaxed geometries are summarized in Table 1, which contains geometries of the perfect and oxygen-vacancy $LaAlO_3(001)$ surfaces with the LaO and AlO_2 terminations. Coordinates are only listed for atoms in the top half of the slab, $z \geq 0$; the others are determined by M_z mirror symmetry. Due to the symmetry, there is no force along x- or y-axis. The layer described in Table 1 is sequentially from the outmost layer inwards.

Table 1. Atomic displacements (relative to ideal positions) of the perfect and oxygen-vacancy surfaces with LaO and AlO_2 terminations (in nm). The positive means the outward displacement of the atoms, while the negative shows their inward motion.

Layer	LaO terminated			AlO_2 terminated		
	Ion	Perfect surface	With oxygen Vacancy	Ion	Perfect Surface	With oxygen vacancy
1	$La^{3+}_{(1)}$	–0.0059	–0.0095	$Al^{3+}_{(1)}$	–0.0059	–0.205
	$O^{2-}_{(1)}$	0.0054	–0.0063	$O^{2-}_{(1)}$	–0.0009	–0.0049
2	$Al^{3+}_{(2)}$	0.0032	–0.0068	$La^{3+}_{(2)}$	0.0077	–0.274
	$O^{2-}_{(2)}$	0.0031	–0.0053	$O^{2-}_{(2)}$	–0.0010	–0.0127
3	$La^{3+}_{(3)}$	–0.0006	–0.0058	$Al^{3+}_{(3)}$	0.0006	–0.0186
	$O^{2-}_{(3)}$	0.0022	–0.0026	$O^{2-}_{(3)}$	–0.0008	-0.0020
4	$Al^{3+}_{(4)}$	0.0005	–0.0039	$La^{3+}_{(4)}$	0.0019	–0.0032
	$O^{2-}_{(4)}$	0.0008	–0.0016	$O^{2-}_{(4)}$	–0.0000	–0.0009

From Table 1, the largest relaxation of the metal atoms in the oxygen-vacancy surface layer can be found to be –0.0095 and -0.0205nm for LaO-terminated and AlO_2-terminated surfaces, respectively. The relaxed geometry for the perfect surfaces is smaller than that of the defect ones in size. However, the difference in the metal atomic relaxation between the perfect and two types of oxygen-vacancy surfaces is noteworthy. It is clear that the oxygen-vacancy makes metal ions shift inwards the second layer of the defect surface structures.

Table 2. Surface relaxation parameters (in percentage of lattice constant). Δd_{12} and Δd_{23} are the changes in the interlayer spacing respectively for the first and second layers, while r_i is the displacement of the oxygen relative to metal atoms in the ith layer of the surface structure.

	Perfect		Oxygen-vacancy		Perfect		Oxygen-vacancy	
	r_1	r_2	r_1	r_2	Δd_{12}	Δd_{23}	Δd_{12}	Δd_{23}
Type I	–3.002	0.023	6.428	2.188	–1.665	1.161	–4.507	0.360
Type II	–1.339	2.312	4.187	10.821	–1.577	0.993	1.559	–3.780

In Table 2, we have compared the structure parameters between the perfect and oxygen-vacancy surfaces with two terminations. Thus, Δd_{12} is defined as the change (relative to bulk) of the first interlayer spacing which is the average z-coordinate measured from the surface to the subsurface; Δd_{23} is defined in a similar way. For the perfect surface, the surface layer is slightly compressed in both terminations. However, for the oxygen-vacancy surfaces, there are different phenomena. The surface layer is seriously collapsed in oxygen-vacancy surface with LaO termination, and it shifts outwards the surface with AlO_2 termination. To quantitate the layer rumpling, the quantity r_i is defined to measure the outward displacement of the oxygen atoms in the ith-layer relative to the other remaining oxygen atoms in the same layer. For the perfect surface with two type terminations, the metal atoms are located above the oxygen atoms,

on the contrary, the oxygen atoms in the two types of surfaces with oxygen vacancies are exposed and there is nothing existing above them.

From the analysis above, it is revealed that the dangling bond in the surface can lead to the relaxation of atoms, and the oxygen-vacancy causes a larger relaxation in the oxygen-vacancy surface. The relaxation might affect the thermal stability and the electronic properties of the system. The thermal stability of LAO films is crucial to the application of high-κ integration, which is studied in the next subsection.

3.2. Surface thermodynamic stability

To compare the energies of surfaces with different stoichiometries, we follow the approach described in Ref.[29]. The relative stabilities of stoichiometric and nonstoichiometric surfaces have to be evaluated in a grand potential Ω. In this framework, the difference in grand potential per 2D unit cell between two terminations is a function of the O chemical potential $\Delta\mu_{\rm O}$, and reads

$$\Delta\Omega = E_{\rm vac}(R) - \Delta N_{\rm O}\Delta\mu_{\rm O}, \tag{1}$$

where the vacancy formation energy $E_{\rm vac}(R)$ for R configuration is defined as

$$\text{with} \quad E_{\rm vac}(R) = E(R+V_{\rm O}) + \frac{1}{2}E[{\rm O}_{2({\rm gas})}] - E(R), \tag{2}$$

$N_{\rm O}$ is the number of missing O atoms per 2D unit cell ($\Delta N_{\rm O}$ is negative in a configuration with these oxygen vacancy), and $\Delta\mu_{\rm O}$ is computed with reference to the total energy per oxygen atom in an oxygen molecule O_2, $\Delta\mu_{\rm O}= \mu_{\rm O} - \frac{1}{2}E[{\rm O}_{2({\rm gas})}]$. In Eq.(2), $E(R+V_{\rm O})$ is the total energy of oxygen-vacancy surface with R termination (R=LaO or AlO_2), $E(R)$ is the total energy of perfect surface with R termination, and $E[{\rm O}_{2({\rm gas})}]$ is the total energy of an oxygen molecule O_2. In our configuration, the formation energies of oxygen-vacancy surface are 6.87eV and 5.10eV for LaO and AlO_2 terminations respectively. The upper bound on $\Delta\mu_{\rm O}$ is obtained on condition that no oxygen condensate forms on the surface ($\Delta\mu_{\rm O} < 0$). Assuming that the $LaAlO_3$ is stable with respect to bulk La, Al and molecular oxygen, the lower bound $\Delta\mu_{\rm O} >$–6.88 eV is obtained (for the bulk $LaAlO_3$, $\mu_{\rm LaAlO3} = \mu_{\rm La} + \mu_{\rm Al} + 3\mu_{\rm O}$). Therefore $\Delta\Omega$ is negative whenever the oxygen deficient surface is more stable than the perfect one.

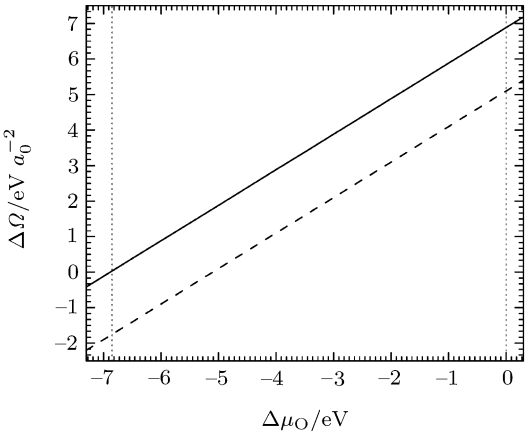


Fig.2. Variations of the thermodynamic grand potential $\Delta\Omega$ with the oxygen chemical potential $\Delta\mu_{\rm O}$ for LaO and AlO_2 termination surfaces with oxygen vacancy. Dotted vertical lines indicate the lower and upper bounds of $\Delta\mu_{\rm O}$ as discussed in the text. The values of $\Delta\Omega$ for the oxygen vacancy surfaces with LaO and AlO_2 terminations are plotted with solid and dashed lines, respectively.

The variations of $\Delta\Omega$ with $\Delta\mu_{\rm O}$ are shown in Fig. 2 for both termination types of $LaAlO_3$(001) surface with oxygen vacancies. From Eq.(1), it is clear that two or more phases with the same oxygen content differ from each other by a quantity independent of $\Delta\mu_{\rm O}$, which is the case for the oxygen vacancy surface with LaO or AlO_2 termination. Furthermore, O-deficient surfaces with AlO_2 termination appear to be less stable than those with LaO termination in a whole allowed range of $\Delta\mu_{\rm O}$. In the O-poor condition, or a low O_2 pressure atmosphere, the value of $\Delta\Omega$ for the AlO_2-terminated surface with oxygen vacancy becomes negative, indicating that the oxygen-vacancy may spontaneously occur.

3.3. Electronic charge redistribution

As is well known, the electronic structure of surface is an important factor to the electrical properties of channel in MOSFET, if a LAO film as a high-κ material is deposited on a semiconductor. Thus, the electronic structure of surface is investigated by analysing the charge redistribution near the surface plane.

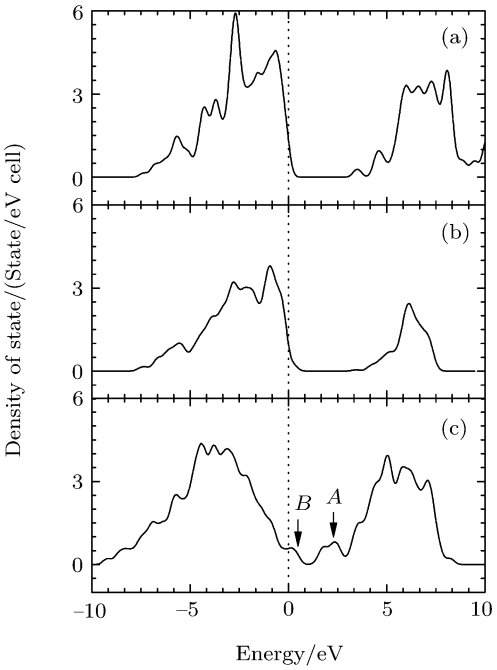


Fig.3. Total density of states in 2D Brillouin zone versus energy for the bulk LAO material (a), perfect LAO surface with AlO_2-termination (b), and oxygen vacancy LAO surface with AlO_2-termination (c).

Figures 3(a)–3(c) show the total densities of states of the bulk $LaAlO_3$, the perfect surface $LaAlO_3(001)$ with AlO_2-termination, and the oxygen-vacancy $LaAlO_3(001)$ surface with AlO_2-termination respectively. Obviously, the optical gap changes slightly for the perfect surface with AlO_2 termination, but considerably for the oxygen-vacancy surface. The peaks A and B lead to a very narrow optical gap, as shown in Fig.3(c). The in-gap states of defect surface with AlO_2 termination exhibit the surface conduction, which may lead to a larger leakage current for the thin film with some oxygen vacancies than that for the bulk material. For the perfect surface, the band gap is slightly reduced, and there are some O 2p states in valence-band intruding upwards into the low part of band gap, especially near the M point of the surface Brillouin zone (the relevant band structure is not given here). These states above the Fermi energy level are due to the surface oxygen atoms, which in the bulk are nearly degenerated, fully occupied and uncharged. While for the perfect $LaAlO_3(001)$ AlO_2-terminated surfaces, the O atoms in the surface layer are not fully occupied by electrons. The unoccupied states make the electronic band structure exhibit some half-filled levels in the valence-band, which contributes to the surface conduction with the hole carriers. These unoccupied states result in the surface states. In the LDA calculation, the unoccupied level is about 0.6eV above the Fermi level, which is at the M point of surface 2D Brillouin zone. Compared with the projected bulk band structure, the band structure of the perfected surface has some distinctions that the top valence band becomes flat near M and Γ points, i.e. the electrons have a larger effective mass. For the conduction band, there appears little change. However, the electronic band structure of the oxygen-vacancy surface is quite different from those of bulk and perfect surfaces. There are some significant groups of bands associated with AlO_2-terminated surface with oxygen-vacancies. First, there are some conduction bands which can shift towards the band gap. They lie above the Fermi level by about 1.8eV. Second, in the top valence-band, near the X points there is a band which crosses the Fermi energy level. Additionally, some states have a tendency to shift upwards the lower band gap, for the imperfect ligand configuration makes the Al 3p orbital distorted at the top layer.

For the LaO-terminated surface, in order to compare the difference in electronic structure between bulk and surface with or without oxygen-vacancy, the total density of states is also plotted, as shown in Figs.4(a)–4(c), respectively. It is clear that the excess electrons of perfect surface have partially filled some conduction bands, while the excess electrons of the oxygen-vacancy surface have fully filled some conduction bands, as indicated by the peak A in Fig.4. For the defect surface, it is shown that F-centre character might contribute to the trapping of electrons by the strong electronic potential around the oxygen-vacancy sites. The electronic band structures of the perfect and oxygen-vacancy $LaAlO_3(001)$ surfaces with LaO termination are obviously different from each other. For the perfect surface, the shapes of the conduction and valence bands are similar, but the Fermi energy level shifts into the conduction bands, especially near the Γ point of the surface Brillouin zone. In addition, the bands at the bottom of conduction-band area are sharper than the ones at the top of valence bands. It means that the electron effective mass is smaller. Moreover, there is no in-gap state in the band structure, which is slightly different from the behaviour of electrons in $BaTiO_3$ surfaces.[30] Our calculation shows that the excess electrons in LaO-terminated surface can result in the shift of Fermi level. For the oxygen-vacancy surface, the definite difference from the perfect surface is that two fold bands shift into the band gap under the Fermi energy level by about

1.0eV. This is caused by the loss of oxygen atoms from the surface. Therefore, the surface becomes metallic, for the excess electrons of the La 6d are localized around oxygen vacancy sites with an imperfect crystalline field.

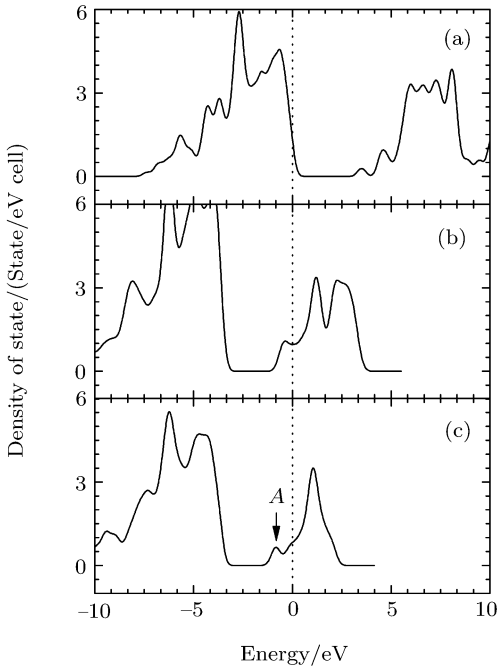


Fig.4. The density of states in 2D Brillouin zone versus energy for the bulk LAO material (a), perfect LAO surface with LaO-termination (b), and oxygen vacancy LAO surface with LaO-termination (c).

4. Conclusion

We have studied the atomic and the electronic structures of the two possible terminated $LaAlO_3$ (001) surfaces with oxygen-vacancy by using the density functional theory and the local density approximation. The results show that the (001) surface exhibits a significant oscillatory geometric relaxation, and the displacement of oxygen-vacancy surface is larger than that of perfect one after relaxation. The size of surface rumpling of LaO-termination with oxygen-vacancy is larger than that of AlO_2-termination. The total density of states shows that the electronic states in the deficient surfaces with different terminations are different. For the LaO-terminated oxygen-vacancy surfaces, the excess electrons can occupy some lower conduction bands. However, some O2p states in the AlO_2-terminated oxygen-vacancy surface become partially occupied in the top of valence bands. The oxygen deficient surfaces exhibit metallic character. From the thermodynamic stability analysis, the different surface thermodynamic grand energies of two slabs with oxygen-vacancy indicate that the AlO_2-terminated oxygen-vacancy surface might be stable.

Acknowledgments

The authors are grateful to Dr X. H. Wei and other co-workers in the State Key Laboratory of Electronic Thin Films and Integrated Devices for their kind help in experiment and useful discussion.

References

[1] Edge L F, Schlom D G, Chamber S A, Cicerrella E, Freeouf J L, Hollnder B and Schubert J 2004 *Appl. Phys. Lett.* **84** 726
[2] Makeev Y G, Motornenko A P, Cherpak N T, Babiichuk I P and Kosmyna M B 2002 *Tech. Phys. Lett.* **28** 221
[3] Park B E and Ishiwara H 2003 *Appl. Phys. Lett.* **82** 1197
[4] Edge L F, Schlom D G, Brewer R T, Chabal Y J, Williams J R, Chambers S A, Hinkle C, Lucovsky G, Yang Y, Stemmer S, Copel M, Hollander B and Schubert J 2004 *Appl. Phys. Lett.* **84** 4629
[5] Lu X B, Lee P F and Dai J Y 2005 *Appl. Phys. Lett.* **86** 203111
[6] Xiang W F, Liu Y Z, Lu H B, Yan L, He M and Chen Z H 2006 *Thin Solid Films* **515** 2722
[7] Xiong K, Robertson J and Clark S J 2006 *Appl. Phys. Lett.* **89** 022907
[8] Pentcheva R and Pickett W E 2006 *Phys. Rev.* B **74** 035112
[9] Asthagiri A and Sholl D S 2006 *Phys. Rev.* B **73** 125432
[10] Knizhnik A A, Iskandarova I M, Bagaturyants A A, Potapkin B V, Fonseca R C and Korkin A 2006 *Phys. Rev.* B **72** 235329
[11] Zhang Ch, Wang Ch L, Li J Ch and Yang K 2007 *Chin. Phys.* **16** 1422
[12] Zhu Zh Y, Wang B, Wang H, Zheng Y, and Li Q K 2007 *Chin. Phys.* **16** 1780
[13] Xiang R Ch, Cheng Y, Hao Y J and Wang Y J 2007 *Chin. Phys.* **16** 217
[14] Xie Y P, Luo Y and Liu Sh J 2007 *Chin. Phys.* **16** 1429
[15] CSun B, Liu Sh J, Duan S Q and Zhu W J 2007 *Acta Phys. Sin.* **56** 1598 (in Chinese)
[16] Shen Y B, Zhou X, Xu M, Ding Y Ch, Duan M Y, Linghu R F and Zhu W J 2007 *Acta Phys. Sin.* **56** 3440 (in Chinese)

[17] Xu L, Tang Ch Q, Dai L, Tang D H and Ma X G 2007 *Acta Phys. Sin.* **56** 1048 (in Chinese)
[18] Hohenberg P and Kohn W 1964 *Phys. Rev.* **136** B864
[19] Kohn W and Sham L J 1965 *Phys. Rev.* **140** A1133
[20] Vanderbilt D 1990 *Phys. Rev.* B **41** 7892
[21] Ceperley D M and Alder B J 1980 *Phys. Rev. Lett.* **45** 566
[22] Perdew J P and Zunger A 1981 *Phys. Rev.* B **23** 5048
[23] Pfrommer B G, Côté M, Louie S G and Cohen M L 1997 *J. Comput. Phys.* **131** 233
[24] Segall M D, Philip J D L, Probert M J, Pickard C J, Hasnip P J, Clark S J and Payne M C 2002 *J. Phys.: Cond. Matt.* **14** 2717
[25] Payne M C, Teter M P, Allan D C, Arias T A and Joannopoulos J D 1992 *Rev. Mod. Phys.* **64** 1045
[26] Monkhorst H J and Pack J D 1976 *Phys. Rev.* B **13** 5188
[27] Geller S and Bala V B 1956 *Acta Crystallogr.* **9** 1019
[28] Kawanowa H, Ozawa H, Ohtsuki M, Gotoh Y and Souda R 2002 *Surf. Sci.* **506** 87
[29] Casek P, Finocchi F and Noguera C 2005 *Phys. Rev.* B **72** 205308
[30] Cai M Q, Zhang Y J, Yin Z and Zhang M Sh 2005 *Phys. Rev.* B **72** 075406